12-8-2014

Reaction Rates of Amino Acids with Derivatives of the Anticancer Drug Cisplatin

Celia Jess Whelan
Western Kentucky University, celia.whelan336@topper.wku.edu

REACTION RATES OF AMINO ACIDS WITH DERIVATIVES OF THE ANTICANCER DRUG CISPLATIN

A Capstone Experience/Thesis Project

Presented in Partial Fulfillment of the Requirements for

The Degree Bachelor of Science with

Honors College Graduate Distinction at Western Kentucky University

By

Celia Jess Whelan

*****

Western Kentucky University
2014

CE/T Committee:

Dr. Kevin M. Williams, Advisor

Dr. Chad A. Snyder

Dr. Ellen W. Bonaguro

Approved by

_____

Advisor
Department of Chemistry

ABSTRACT

We are studying reactions of cisplatin derivatives, which differ in both size and shape, with various amino acids. When reaction with DNA occurs, apoptosis is observed, ideally leading to termination of the cancer. Due to the affinity of cisplatin for sulfur-containing amino acids, reaction with proteins may occur prior to access to the DNA, producing a large array of products, which could potentially be toxic to the human body. Both the size and shape of the platinum complexes often affect the reactions with protein targets more so than with DNA targets. By performing reactions of specific amino acids targets with our cisplatin derivatives, we attempt to understand the factors that influence the targeting of these specific amino acids. In this study, cisplatin derivatives have been reacted with the amino acids histidine, cysteine, and methionine, and the reactions have been monitored by NMR spectroscopy, and rate constants calculated using DYNAFIT. It has been seen that adding bulk to the ligands of our platinum compounds has little to no effect on the reaction with histidine compared with methionine and cysteine targets. Thus, sufficient bulk may increase the relative number of histidine adducts compared with methionine or cysteine adducts, consequently decreasing the toxic side effects experienced by users of the drug.

Keywords: Cisplatin, Histidine, Cysteine, Methionine, Anticancer, Nuclear Magnetic Resonance

Dedicated to my friends, family, and professors who have always encouraged me

ACKNOWLEDGEMENTS

This project would not have been possible without the help and support of so many people. I am so incredibly thankful for all the support, encouragement, and knowledge of Dr. Kevin Williams, my research advisor, over the past several years. I would also like to thank Dr. Snyder, Dr. Dahl, Dr. Pesterfield, Alicia Pesterfield, and Dr. B for all of the laughs, the advice, and the inspiration to keep going and pursue my dreams.

I would also like to thank the Honors College for providing an intellectual environment in which I was able to grow as a scholar. In addition, I would like to thank the Office of Research for the FUSE Grant. I would also like to thank the NIH and RCAP for the grants that allowed me to do the majority of the research over my first four years in the lab. Without the help of all the funding my lab has received, I would not have been able to complete this project.

Finally, I would like to thank my friends and family. Thanks to my Mom and Dad for always supporting me and encouraging me in everything that I do, and to my friends who have always helped me to keep going when I thought I couldn't go any more. I appreciate the love and encouragement from every single one of you.

VITA

January 25, 1993……	Born – Louisville, Kentucky
2011……...……	Bardstown High School, Bardstown, Kentucky
2011……...……	Carol Martin Gatton Academy of Mathematics and Science in Kentucky, Bowling Green, Kentucky
2012……...	NSF REU at Western Washington University, Bellingham, Washington

PUBLICATIONS

1. R. S. Sandlin; C. J. Whelan; M. S. Bradley; K. M. Williams. *Inorganica Chimica Acta* **2012**, *391*, 135-140

FIELDS OF STUDY

Major Fields: Chemistry (ACS Certified), Communication Studies

Minor Fields: Mathematics, Music (Vocal Performance)

TABLE OF CONTENTS

TABLE OF FIGURES

CHAPTER 1

INTRODUCTION

Cancer is something that affects every person in the world in some way, shape, or form. Whether young or old, gay or straight, man or woman, almost every person knows someone who has, had, or will have cancer. In 2014 alone, it is estimated that 585,720 cancer-related deaths will occur in the United States, nearly 15,000 of which are expected to be due to ovarian cancer [1]. While many anticancer drugs have been developed for a myriad of different cancers, one commonly used chemotherapeutic in combatting ovarian cancer is cisplatin, which is also used to fight testicular, lung, bladder, and other cancers [2].

Cisplatin, or *cis*-diaminedichloroplatinum(II), was first discovered to have anticancer activity by the Rosenberg lab at Michigan State University in 1965 [3]. This discovery was entirely on accident as the lab was experimenting with the effect of a generated electric field, using platinum electrodes, on the growth and division of *E. coli* cells [3]. During this experiment, it was observed that the *E. coli* cells were growing, but the cells were not dividing. This eventually led to the hypothesis that this inhibition was due to the products of the platinum electrode hydrolysis [3]. The lab then discovered that several different products were being produced by the platinum electrode hydrolysis which could be responsible for the inhibition of the cell division [3].

Following this, Rosenberg began to test the ability of the platinum compounds to eliminate or reduce implanted solid Sarcoma-180 tumors in mice [3]. The results of these assays indicated two things: one, that platinum(II) complexes exhibited the most ability to reduce the mass of the cancerous tumors, and second, that the observed biological effects were stereospecific [3]. These platinum(II) complexes can be found in both the *cis*- and *trans*- isomeric forms. Complexes which exhibit anticancer activity are in the *cis*- isomeric form; those in the *trans*- form are largely anticancer inactive. Thus cisplatin, *cis*-$[Pt^{II}(NH_3)_2Cl_2]$, was the platinum electrode hydrolysis product which was responsible for the anticancer activity and the first platinum-containing anticancer drug to become FDA approved – which occurred in 1971 [3]. Transplatin, *trans*-$[Pt^{II}(NH_3)_2Cl_2]$, was discovered to be anticancer inactive.

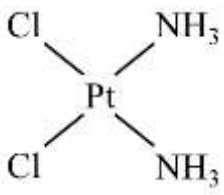

Figure 1.1. Structure of cisplatin.

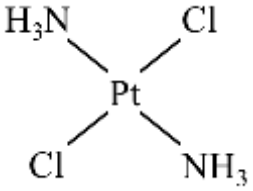

Figure 1.2. Structure of transplatin.

N,N'-ethylenediamine	en
N,N,N',N'-tetramethylethylenediamine	Me_4en
N-acetyl-methionine	*N*-AcMet
N-acetyl-histidine	*N*-AcHis
N-acetyl-cysteine	*N*-AcCys
Deoxyribonucleic acid	DNA
Copper transporter 1	CTR1
Oxalate	ox

Unfortunately, cisplatin showed some severe dose-limiting side effects including nephrotoxicity – severe kidney damage – to the patient and this spawned the search for other platinum-based anticancer drugs which were just as effective as cisplatin in terms of combatting cancer, but caused far fewer side effects. Following first-generation cisplatin, second-generation carboplatin was developed, and since that time there have been thousands of platinum drug derivatives created and tested for their anticancer activity in the hopes of creating a better drug [4]. From all of these options, only third-generation oxaliplatin along with carboplatin and cisplatin, have been approved for international marketing [5], though others, such as phenanthriplatin, have shown promise in clinical trials. In order to become FDA approved, that drug must show at least one advantage over cisplatin. Both carboplatin, FDA approved in 1989 [6], and oxaliplatin, FDA approved in 2002 [5], are effective against cancer cell lines that are cisplatin-resistant. Carboplatin is predominately used in the combat of ovarian cancer [5] but is also used to treat non-small cell lung and other cancers [6], while oxaliplatin is more commonly used in cases of colorectal cancer [5].

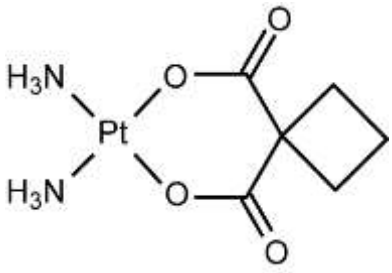

Figure 1.3. Structure of carboplatin.

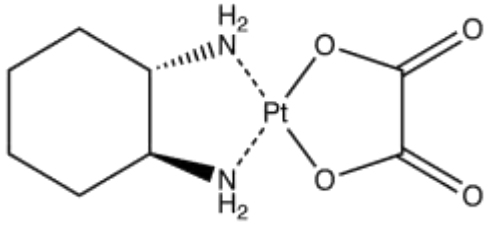

Figure 1.4. Structure of oxaliplatin.

Regrettably, both carboplatin and oxaliplatin present severe dose-limiting side effects as well, though they are different from those of cisplatin. While nephrotoxicity was one of the dominant side effects caused by cisplatin, carboplatin tends to cause myelosuppression – an extreme decrease in bone marrow activity causing a reduction in both red and white blood cells as well as platelets – and oxaliplatin is guilty of causing neurotoxicity – interfering with the normal activity of the nervous system [5]. Thus, it should come as no surprise that the hunt for a more effective and less toxic anticancer drug continues today.

One of the believed causes for some of the severe side effects experienced by cisplatin-users is the sulfur-platinum(II) binding [7]. Because sulfur is quite abundant in the human body, present in biomolecules such as glutathione and amino acids cysteine and methionine to name a few, there is thus a high probability for these sulfur-platinum(II) bonds to be formed. Many studies suggest that within 24 hours of cisplatin administration, roughly between 65% and 98% of the cisplatin has been sequestered by proteins [7]. This is unfortunate for two reasons: first, the most common way to deactivate the platinum-drug is for it to form a protein adduct, and second, protein adducts are most commonly formed through by sulfur-platinum(II) bonding. So, not only does the drug become less potent because much of it is deactivated, this deactivation through a sulfur-platinum(II) bonded protein adduct is thought to be toxic to the patient.

Though the platinum center of cisplatin has an affinity for sulfur, the anticancer mechanism of cisplatin is dependent on the drug being able to enter the cancerous cells and bond with the DNA; in order to do this the drug must first be uptaken into the cancerous cell. While the uptake method of cisplatin in not entirely understood, studies

suggest that both passive diffusion and use of CTR1 play a key role in drug uptake [4, 7, 8], neither of which can occur if the drug is protein-bound. Many of the earlier studies on the topic of cisplatin uptake suggest that unaquated cisplatin – meaning the two chlorines are bonded to the platinum center, shown in Figure 1.1 – passively diffuses through the cell membrane into the tumor cell [4, 7]. More recent research has shown that cisplatin may be actively transported into the cell via CTR1 [4, 8]. CTR1 is a transmembrane copper transporter containing a central trimeric pore composed of histidines, methionines, and cysteines. As previously stated, the platinum center has an affinity for sulfur, thus making the pore of CTR1 an attractive binding option. The use of CTR1 to transport platinum drugs into cells is evidenced by studies which have found that the deletion, or even mutation, or the CTR1 gene causes an increase in cell resistance to cisplatin while an overexpression of the gene causes an increase in platinum drug concentration within the cells [4, 8]. Thus, it can be said that the cytotoxicity of cisplatin seems to be regulated by CTR1.

Outside of the cell, the drug remains in its unaquated form due to the extremely high concentrations of chloride ion ($[Cl^-] \approx 100$ mM), but once it is inside the cell the chloride concentration is much lower ($[Cl^-] \approx 4$ mM) and the drug becomes aquated – meaning that the chlorine atoms of cisplatin are displaced by water, H_2O [7]. Cisplatin first becomes mono-aquated, *cis*-$[Pt^{II}(NH_3)_2(H_2O)Cl]^+$ – where only a single chlorine is displaced – and finally bis-aquated, *cis*-$[Pt^{II}(NH_3)_2(H_2O)_2]^{2+}$ – both chlorines displaced by water. This aquation process is important because once the drug becomes positively charged it cannot leave the cell and can diffuse into the cell's nucleus where it can bind

with the DNA. Roughly 98% of the DNA-platinum adducts are formed from the mono-aquated species, though there are other DNA-platinum adducts that can form as well [7].

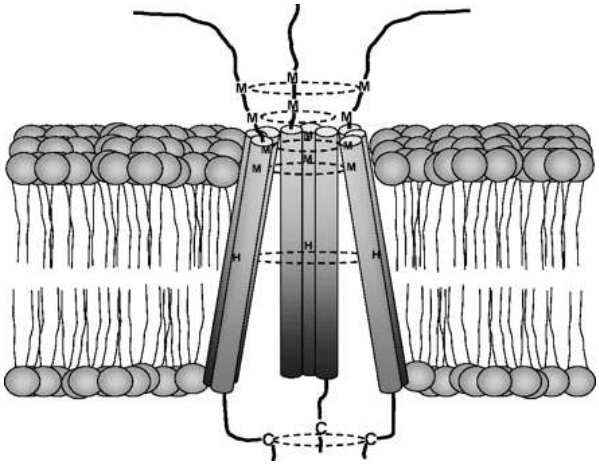

Figure 1.5. Homotrimeric pore of the transmembrane CTR1 where M indicates methionine, C indicates cysteine, and H indicates histidine [8].

Cisplatin is anticancer active due to the way that the aquated forms interact with cancerous cell DNA. As Figure 1.6 indicates, there are several ways that cisplatin can bind with the DNA in order to damage it: both inter- and intra-strand crosslinks, as well as a protein-DNA crosslink. Once inside the nucleus, the central platinum atom binds with the N^7 atoms of the DNA bases guanine and adenine, though guanine is preferred [4, 9]. The most common DNA adduct produced is that of the intra-strand crosslink, either the 1,2, which typically occurs between two adjacent guanines, or the 1,3, which binds to guanines in a GXG sequence where X is another DNA base. Adjacent guanine residues are preferred because this region is the most electronegative of the double-stranded DNA, and thus the positively charged aquated product targets this region [9]. While adjacent

guanines residues are preferred, an adenine residue in conjunction with a guanine residue can also produce crosslinks. But it should be noted that all DNA adducts, not solely the intra-strand crosslinks, play a role in the drug's toxicity [4, 9].

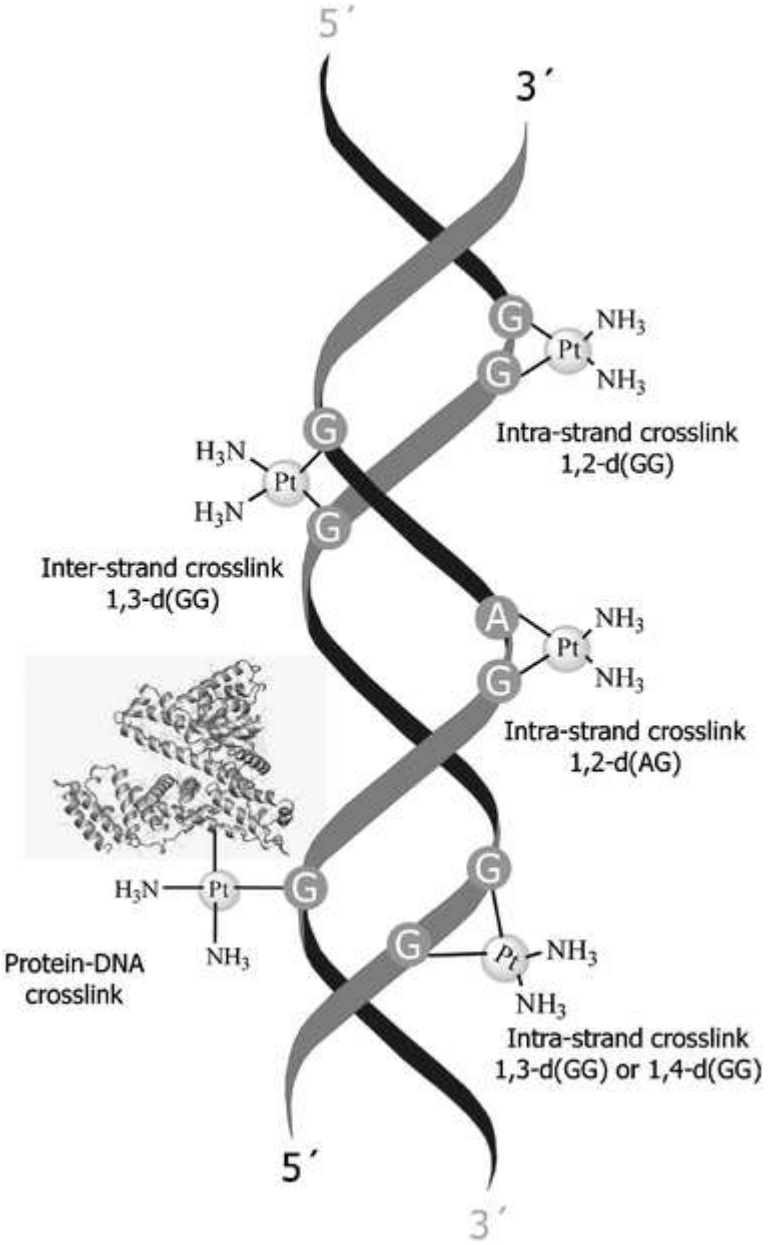

Figure 1.6. Visual depiction of possible crosslinks that can be produced by aquated species [10].

Ideally, these crosslinks kink the DNA in such a way that the repair proteins cannot fix the DNA and cell death is triggered. The 1,2-intrastrand crosslink in particular distorts the DNA in such a way that the DNA's minor groove is exposed, revealing the area where several different classes of proteins can bind, such as high-mobility group (HMG) box, repair and transcription proteins [4]. The HMG proteins are preferential toward platinum-guanine adducts, and specific proteins such as HMGB1 bind to the platinum-guanine adduct in order to protect it from repair proteins [4]. This DNA damage induces cell cycle arrest which then prompts apoptosis – cell death. It is the inability of transplatin to form these types of crosslinks which accounts for its anticancer inactivity.

While the main targets of these platinum-containing drugs are DNA, much of the drug is sequestered by proteins and other biomolecules before it reaches the cancer cell DNA. Since these proteins are found in places such as the blood it is extremely important to understand these reactions and how they change as the drug derivative changes. The focus of our research is on understanding how the reactions between cisplatin derivatives and certain amino acids found within proteins change depending on the size and shape of the attached ligands. In other words, we want to understand how much bulk can be added to these drugs before severe retardation of the reaction rate is observed. In this research, we will specifically focus on the acetylated forms of three amino acids – cysteine (Figure 1.8), methionine (Figure 1.7), and histidine (Figure 1.9) – and how added bulk on both the leaving and carrier ligands of the drug will affect the reaction rates with these amino acids. We will also be looking at which products are formed during each of these reactions.

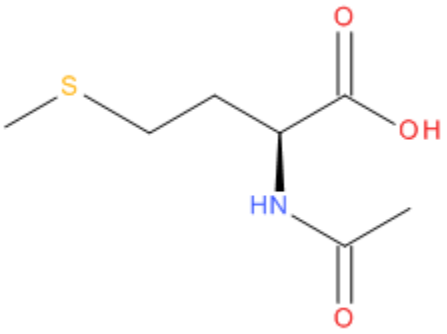

Figure 1.7. Structure of *N*-AcMet

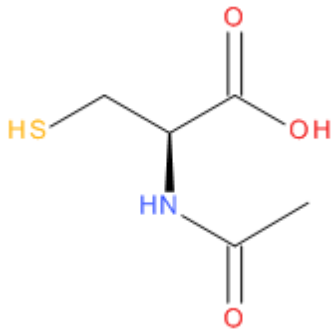

Figure 1.8. Structure of *N*-AcCys

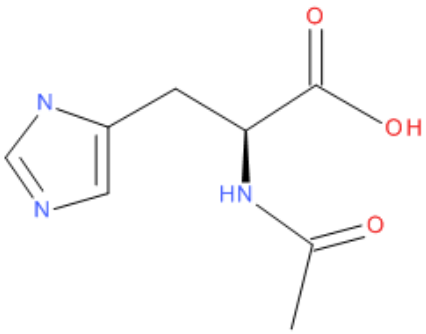

Figure 1.9. Structure of *N*-AcHis

There are several reasons these three amino acids were chosen for investigation into their reactions with platinum drug derivatives. First, as stated previously, platinum drug reaction with sulfur-containing biomolecules is believed to be one of the causes of toxicity; both methionine and cysteine are sulfur containing amino acids found in many proteins and are both responsible for sequestration of platinum-containing anticancer

drugs. Therefore it is imperative to study the products formed in these reactions. In addition, it is necessary to investigate the reaction rates of platinum-containing drugs with these three amino acids because they compose the trimeric pore of CTR1, which partially regulates drug uptake into the cancerous cells. Therefore, we need to evaluate whether or not our drug derivatives still possess a reaction rate fast enough to allow the drug to be transported into the cancer cells.

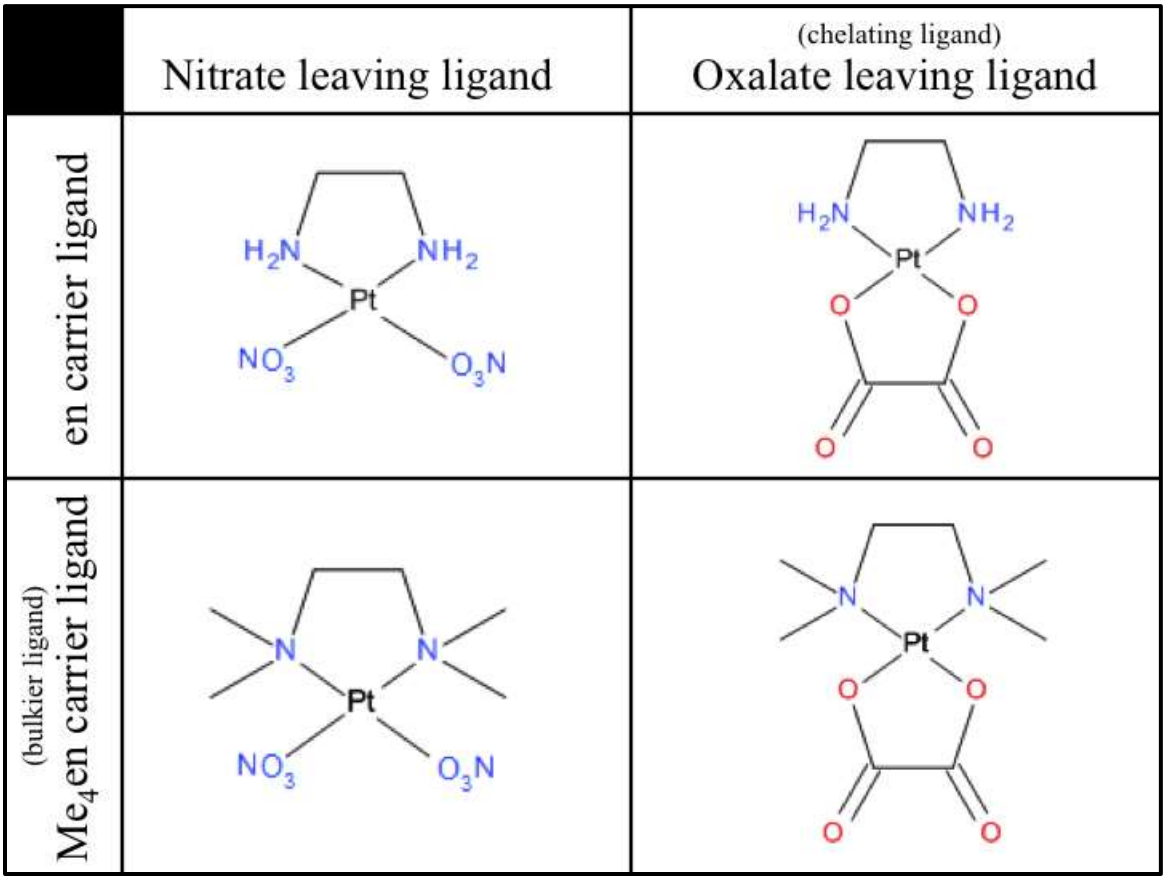

Figure 1.10. Visual representation for the split between bulkier carrier and leaving ligands, and structures for the four compounds used in this research.

In this case we have chosen to use four different cisplatin drug derivatives. Two derivatives have nitrate leaving ligands, and two have oxalate leaving ligands; one of those with the nitrate leaving ligand has an en carrier ligand and the other an Me_4en carrier ligand, and the same trend holds for those with the oxalate leaving ligand. A visual representation, including structures for each of the cisplatin derivatives used in this research, of this can be found in Figure 1.7. We expect that as the bulk of the platinum compound increases, the reaction rate with respect to one amino acid will slow down. In addition, we expect that as the leaving ligand is changed from a non-chelating ligand (nitrate) to a chelating ligand (oxalate), the reaction rate with respect to one amino acid will decrease; this is due to the chelate effect. First of all, a chelate is any ligand that binds to the metal center through more than one atom. So in this case, en, Me_4en, and oxalate are all chelates. Secondly, the chelate effect is the concept that chelated compounds are more stable than non-chelated compounds and thus the greater the number of chelates, the more thermodynamically stable the compound will be.

What we have found is, for the most part, what we expected. In terms of methionine, adding bulk to the carrier ligand of the compound greatly reduced the rate of reaction; this holds for cysteine as well. What was interesting was our finding in relation to histidine and rate of reaction as bulk is increased on the carrier ligand and a chelating leaving ligand is used. In terms of the nitrate leaving ligands, there was negligible difference between the reaction rates with histidine as we varied the carrier ligand [11]. But as we replace the nitrate leaving ligand with oxalate, while keeping the carrier ligand the same, the reaction rate with histidine is so retarded that product formation is negligible even after 14 months of reaction time. This indicates that increasing the bulk

of the carrier ligands would reduce the rate of reaction with both cysteine and methionine, while the reaction with histidine would not change. In addition, we now know that by adding a chelating leaving ligand to our platinum drug derivative, the reaction rate with histidine retards so greatly that reaction is considered not to have occurred.

CHAPTER 2

MATERIALS AND METHODS

The following chemicals were purchased for use in syntheses performed for this research:

Deuterium oxide (D_2O) (Aldrich, 99.9 atom % D), Potassium tetrachloroplatinate(II) (Aldrich, 98%), Ethylenediamine (Acros, p.a.), N,N,N',N'-tetramethylethylenediamine (Acros, 99%), Oxalic acid (Acros, anhydrous p.a.), Silver nitrate (Sigma-Aldrich, ≥99.0%), Potassium iodide (Sigma-Aldrich, 99+%, A.C.S. reagent), Acetone (Sigma-Alrich, Histological grade, ≥99.5%), Methanol (Sigma-Aldrich, HPLC grade, ≥99.9%), dichloro(ethylenediamine)platinum(II) (Alrich, 99%), *N*-Acetyl-L-cysteine (Acros, 98%), *N*(alpha)-Acetyl-L-histidine monohydrate (Acros, 99+%), *N*-Acetyl-L-methionine (Fluka Analytical, ≥98.5%).

All synthesis products were checked for purity using a JEOL Eclipse 500 MHz nuclear magnetic resonance (NMR) spectrometer and collecting ^1H NMR spectra. In each case, deuterium oxide (D_2O) was used as a standard reference. The following syntheses were commonly used:

Synthesis of diiodo(ethylenediamine)platinum(II):

430 mg of potassium tetrachloroplatinate(II) was combined with 1315 mg of potassium iodide (excess) in approximately 5 mL of deionized water. After approximately 3 hours, the reaction mixture was syringe filtered into a round bottom flask and 167 µL of ethylenediamine ligand was added dropwise and another 5 mL of deionized water added. The reaction was allowed to stir overnight and a yellow mustard colored precipitate was noted. The solution was vacuum filtered in order to collect the precipitate. The solid was washed once with deionized water, then ethanol, and then diethyl ether. Once dry, the solid was collected. Yield = 486.2 mg.

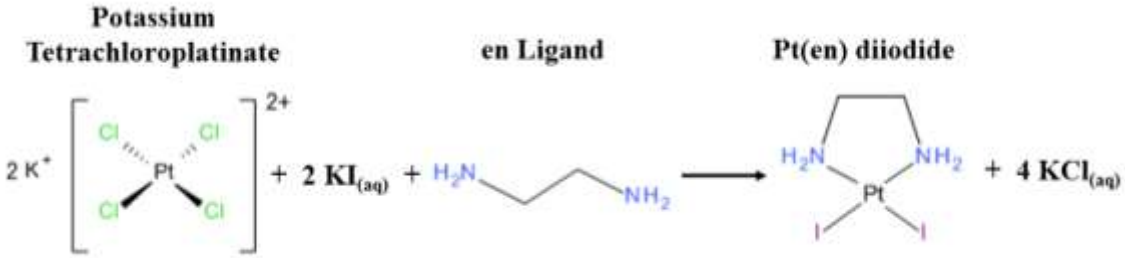

Figure 2.1. Synthesis of Pt(en) diiodide

Synthesis of diiodo(N, N, N', N'-tetramethylethylenediamine)platinum(II):

464.5 mg of potassium tetrachloroplatinate(II) was combined with 1303 mg of potassium iodide (excess) in approximately 5 mL of deionized water. After approximately 3 hours, the reaction mixture was syringe filtered into a round bottom flask and 375 µL of (N,N,N',N'-tetramethylethylenediamine) ligand was added dropwise and another 5 mL of deionized water was added. The reaction was allowed to stir overnight and a brown mud-colored precipitate was noted. The solution was vacuum filtered in order to collect the precipitate. The solid was washed once with deionized water, then ethanol, and then diethyl ether. Once dry, the solid was collected. Yield = 534.6 mg.

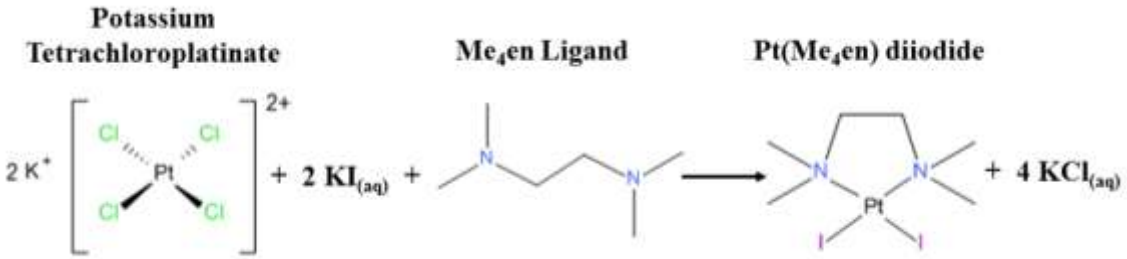

Figure 2.2. Synthesis of Pt(Me_4en) diiodide

Synthesis of (N, N'-ethylenediamine)platinum(II) nitrate:

103.0 mg of previously synthesized diiodo(N,N'-ethylenediamine)platinum(II) was added to an aluminum foil-covered Erlenmeyer flask containing approximately 150 mL of acetone, which was swirled until the platinum compound was completely dissolved. Then, 69.2 mg of silver nitrate was added to solution and the reaction was allowed to stir overnight. Gravity filtration was then performed in order to remove the precipitate and the filtrate was collected in a round bottom flask. The solvent was then rotary evaporated off and the remaining solid product collected and weighed. Yield = 66.9 mg.

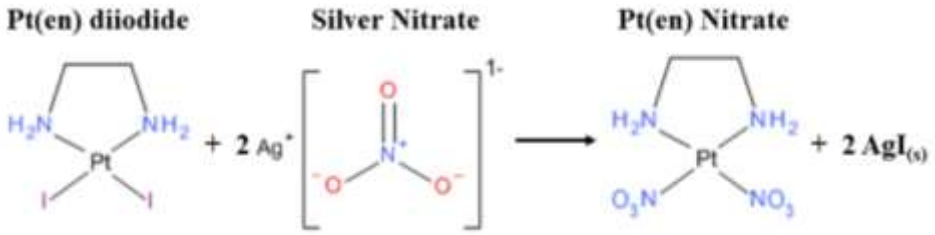

Figure 2.3. Synthesis of Pt(en) Nitrate

Synthesis of (N, N, N', N'-tetramethylethylenediamine)platinum(II) nitrate:

25.5 mg of previously synthesized diiodo(N,N,N',N'-tetramethylethylenediamine)platinum(II) was added to an aluminum foil-covered Erlenmeyer flask containing approximately 15 mL of acetone, which was swirled until the platinum compound was completely dissolved. Then, 15.3 mg of silver nitrate was added to solution and the reaction was allowed to stir overnight. Gravity filtration was then performed in order to remove the precipitate and the filtrate was collected in a round bottom flask. The solvent was then rotary evaporated off and the remaining solid product collected and weighed. Yield = 8.9 mg.

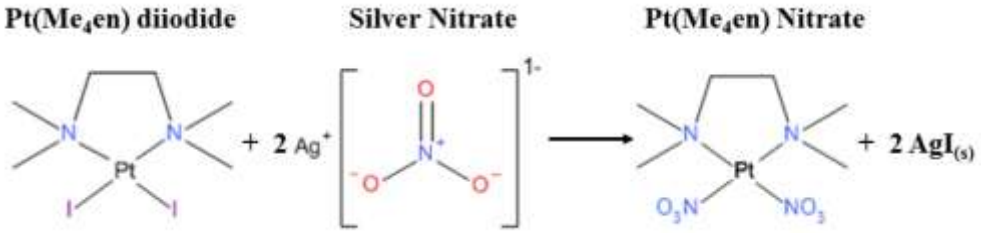

Figure 2.4. Synthesis of Pt(Me_4en) Nitrate

Synthesis of Silver Oxalate:

500.2 mg of silver nitrate was added to aluminum foil-covered Erlenmeyer flask containing approximately 25 mL of deionized water. Next, 149.9 g of oxalic acid was added to the flask and was allowed to stir overnight and a white precipitate was noted. Gravity filtration was then performed in order to collect the white solid precipitate. Once dried, the precipitate was collected and weighed and then stored in the dark.

Yield = 376.1 mg.

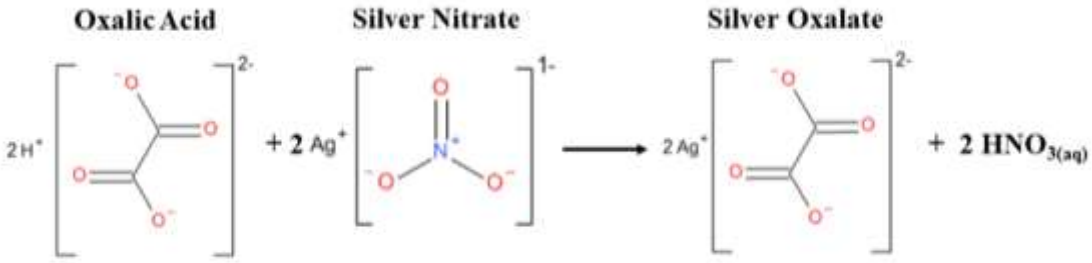

Figure 2.5. Synthesis of silver oxalate

Synthesis of (N, N'-ethylenediamine)platinum(II) oxalate:

35.1 mg of dichloro(ethylenediamine)platinum(II) was placed in an aluminum foil-covered Erlenmeyer flask in 45 mL of deionized water. 33.0 mg of previously synthesized silver oxalate was added and the reaction was allowed to stir in the dark over night. Gravity filtration was then performed in order to remove excess solid and the filtrate collected in a round bottom flask. The round bottom was then placed on a rotary evaporator, in order to remove the solvent, and in a 45°C water bath, in order to ensure ligand coordination. The solid product was then weighed and stored. Yield = 25.6 mg.

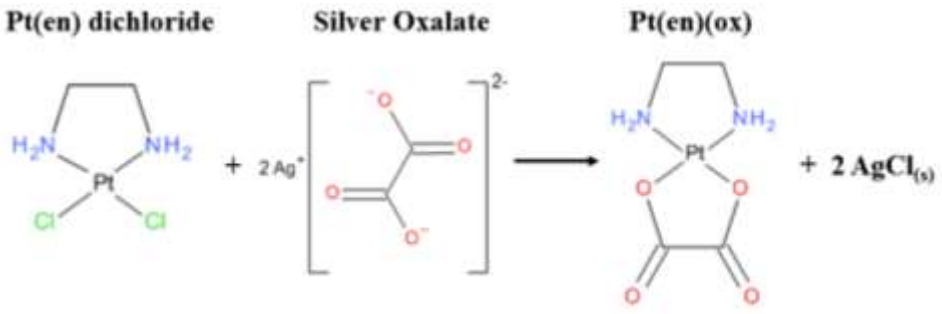

Figure 2.6. Synthesis of Pt(en)(ox)

Synthesis of dichloro(N, N, N', N'-tetramethylethylenediamine)platinum(II):

Solution A: 5 mL of methanol was mixed with 85 μL of (N,N,N',N'-tetramethylethylenediamine) ligand in a 10 mL glass vial.

Solution B: 5 mL of deionized water and 167.5 mg of potassium tetrachloroplatinate (II) were mixed in a 10 mL glass vial.

Next, solution **A** was added *DROPWISE* to solution **B** and there was a noted color change from yellow to orange. The reaction was allowed to stir overnight and a precipitate was formed. The solution was then transferred to a round bottom flask, and a rotary evaporator was used to removed the solvent. The solid product was then collected and weighed. Yield = 45.1 mg.

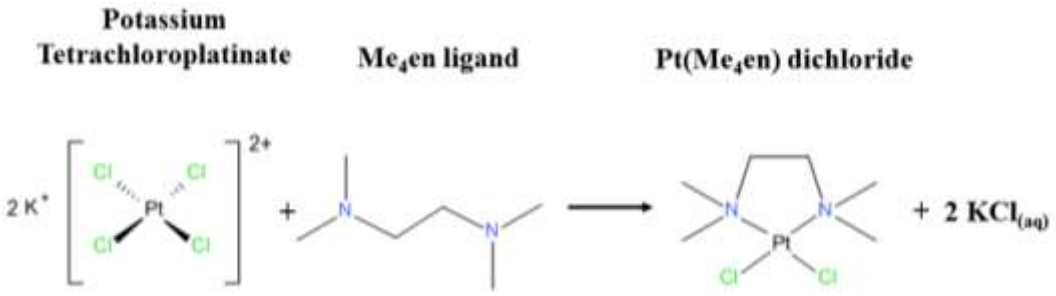

Figure 2.7. Synthesis of Pt(Me_4en) dichloride

Synthesis of (N, N, N', N'-tetramethylethylenediamine)platinum(II) oxalate:

39.9 mg of previously synthesized dichloro(N,N,N',N'-tetramethylethylenediamine)platinum(II) was placed a 40 mL amber vial with approximately 40 mL of deionized water. 30.4 mg of silver oxalate was then added and the reaction was allowed to stir over night. The solution was then gravity filtered in order to remove any excess solid and the filtrate was collected in a round bottom flask. The round bottom was then placed on a rotary evaporator, in order to remove the solvent, and in a 40°C water bath, in order to ensure ligand coordination. The solid product was then weighed and stored. Yield = 20.3 mg.

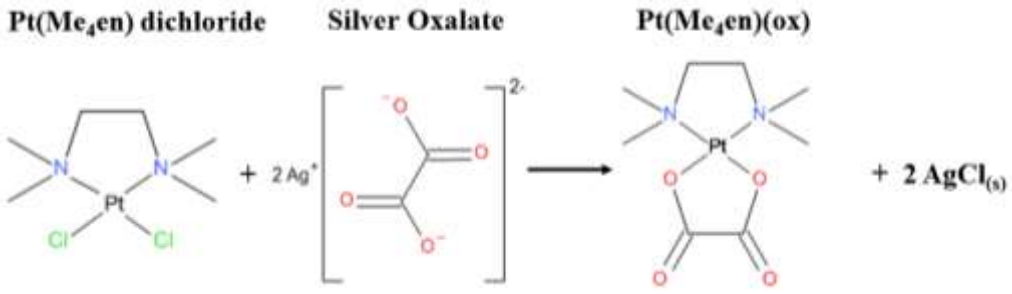

Figure 2.8. Synthesis of Pt(Me_4en)(ox)

All reactions were monitored using a JEOL Eclipse 500 MHz nuclear magnetic resonance (NMR) spectrometer and collecting ^{1}H NMR spectra at selected intervals of time, either manually or via use of a kinetics module.

The following reactions were performed in the specified concentrations at the adjusted pH and then monitored via ^{1}H NMR to determine reaction kinetics and observe products:

Pt(en)$(NO_3)_2$ + *N*-AcMet:

1:1 Pt:*N*-AcMet molar ratio – 10 mM stock solutions of Pt(en)$(NO_3)_2$, *N*-AcMet, and sodium nitrate were prepared in D_2O. 100 μL of Pt(en)$(NO_3)_2$ stock solution, 100 μL of *N*-AcMet stock solution, 100 μL of sodium nitrate stock solution, and 700 μL of D_2O were combined in a clean NMR tube and the pH was adjusted to 4.

Pt(en)$(NO_3)_2$ + *N*-AcHis:

1:1 Pt:*N*-AcHis molar ratio – 10 mM stock solutions of Pt(en)$(NO_3)_2$, *N*-AcHis, and sodium nitrate were prepared in D_2O. 100 μL of Pt(en)$(NO_3)_2$ stock solution, 100 μL of *N*-AcHis, 50 μL of sodium nitrate stock solution, and 200 μL of D_2O were combined in a clean NMR tube. The pH was adjusted to 4.

1:2 Pt:*N*-AcHis molar ratio – 10 mM stock solutions of Pt(en)$(NO_3)_2$, *N*-AcHis, and sodium nitrate were prepared in D_2O. 100 μL of Pt(en)$(NO_3)_2$ stock solution, 200 μL of

N-AcHis, 50 μL of sodium nitrate stock solution, and 100 μL of D_2O were combined in a clean NMR tube. The pH was adjusted to 4.

30:5 Pt:*N*-AcHis molar ratio – 40 mM stock solutions of $Pt(en)(NO_3)_2$, *N*-AcHis, and sodium nitrate were prepared in D_2O. 450 μL of $Pt(en)(NO_3)_2$ stock solution, 75 μL of *N*-AcHis, and 75 μL of sodium nitrate stock solution were combined in a clean NMR tube. The pH was adjusted to 4.

$Pt(Me_4en)(NO_3)_2$ + *N*-AcHis:

30:5 Pt:*N*-AcHis molar ratio – 40 mM stock solutions of $Pt(Me_4en)(NO_3)_2$, *N*-AcHis, and sodium nitrate were prepared in D_2O. 450 μL of $Pt(Me_4en)(NO_3)_2$ stock solution, 75 μL of *N*-AcHis, and 75 μL of sodium nitrate stock solution were combined in a clean NMR tube. The pH was adjusted to 4.

1:1 Pt:*N*-AcHis molar ratio – 5 mM stock solutions of $Pt(Me_4en)(NO_3)_2$ and *N*-AcHis were prepared in D_2O. 300 μL of $Pt(Me_4en)(NO_3)_2$ stock solution and 300 μL of *N*-AcHis stock solution were combined in an NMR tube.

Pt(en)(ox) + *N*-AcHis:

1:1 Pt:*N*-AcHis molar ratio – 5 mM stock solutions of Pt(en)(ox) and *N*-AcHis were prepared in D_2O. 300 μL of Pt(en)(ox) stock solution and 300 μL of *N*-AcHis stock solution were combined in a clean NMR tube. The pH was adjusted to either 4 or 7 as required for the experiment.

Pt(en)(ox) + *N*-AcCys:

1:1 Pt:*N*-AcCys molar ratio – 5 mM stock solutions of Pt(en)(ox) and *N*-AcCys were prepared in D_2O. 300 μL of Pt(en)(ox) stock solution and 300 μL of *N*-AcCys were combined in a clean NMR tube. The pH was adjusted to either 4 or 7 as required for the experiment.

Pt(Me_4en)(ox) + *N*-AcCys:

1:1 Pt:*N*-AcCys molar ratio – 5 mM stock solutions of Pt(Me_4en)(ox) and *N*-AcCys were prepared in D_2O. 300 μL of Pt(Me_4en)(ox) stock solution and 300 μL of *N*-AcCys were combined in a clean NMR tube. The pH was adjusted to 7.

Depending on the accuracy of rate constant needed for each reaction, the rate constant was either estimated or determined using DYNAFIT software and the collected ^{1}H NMR spectra.

CHAPTER 3

RESULTS

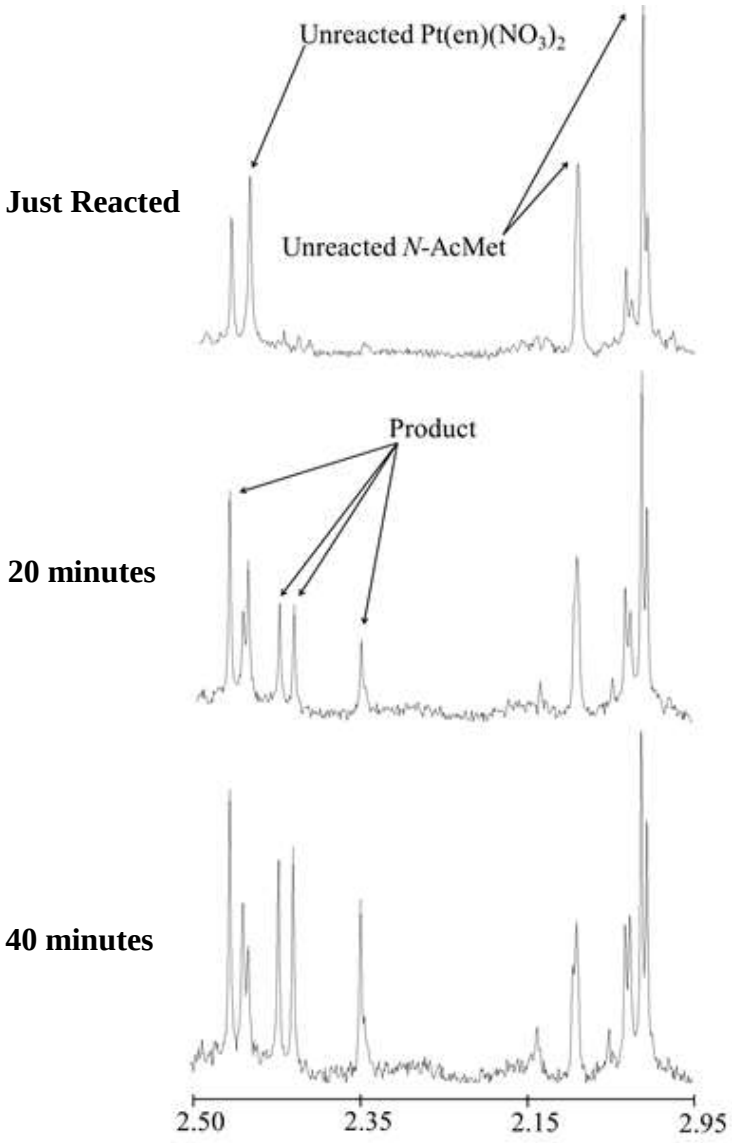

Figure 3.1. Partial ^{1}H NMR spectra of the reaction of 1 mM $Pt(en)(NO_3)_2$, 1 mM sodium nitrate, and 1 mM N-AcMet with a total reaction time of 60 minutes at pH 4 and 25 °C. The peaks associated with reactant and products are indicated, and the y-axis has been scaled to the highest peak. The x-axis is measured in ppm.

The unreacted *N*-AcMet has two prominent singlets at roughly 2.0 ppm and 2.1 ppm, and the prominent singlet at approximately 2.45 is associated with the $Pt(en)(NO_3)_2$. Upon product formation, there are four signals indicated in the middle spectra of Figure 3.1. The singlet at 2.45 and the doublet between 2.4 and 2.45 ppm more than likely indicates the formation of the $[Pt(en)(N\text{-AcMet-S,N})]^+$ chelate. The remaining singlet at 2.35 ppm is associated with the hydrogens of the $S\text{-}CH_3$ group. The rate constant for this reaction was calculated using DYNAFIT and was determined to be $3.8 \pm 0.7\ M^{-1}\ s^{-1}$ [11].

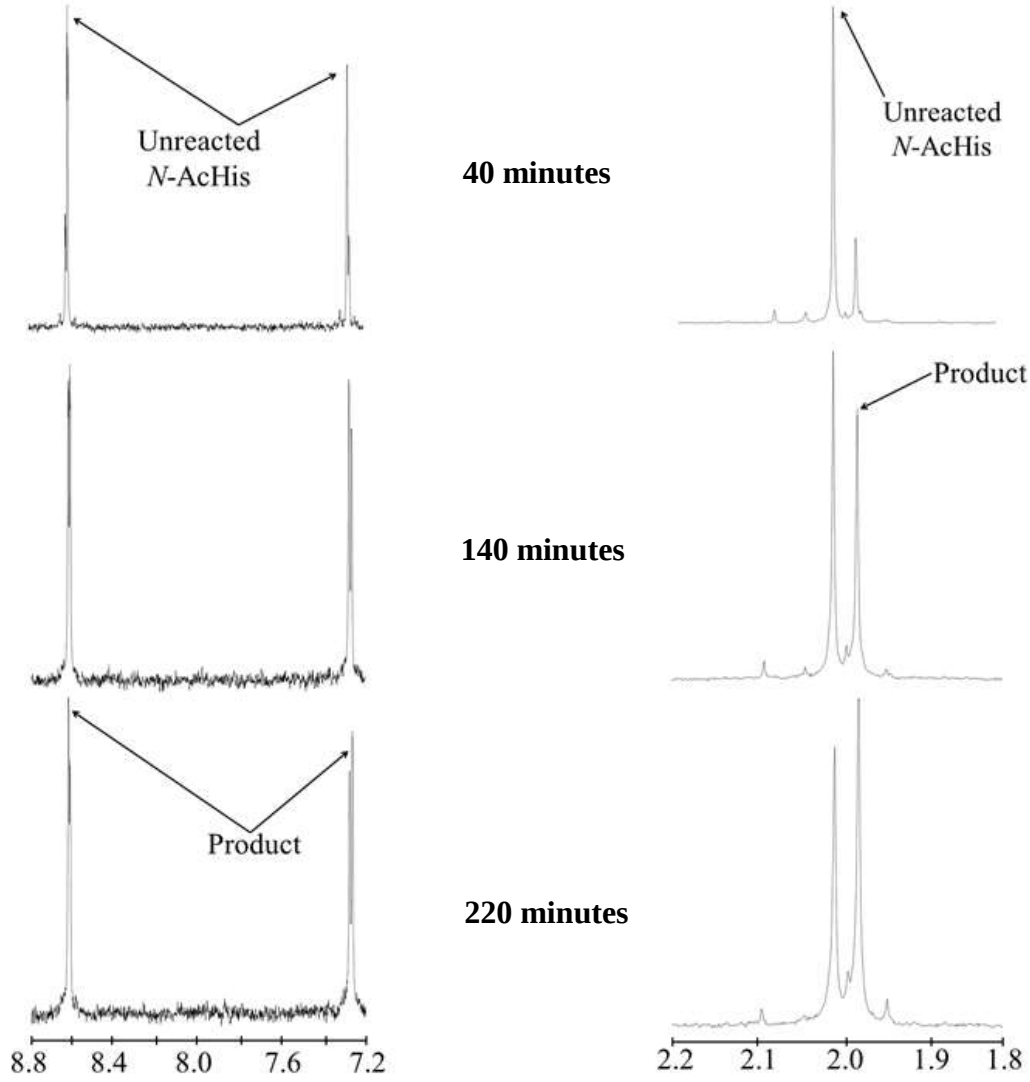

Figure 3.2. The downfield (left) and upfield (right) partial ^{1}H NMR spectra of the reaction of 30 mM Pt(en)$(NO_3)_2$ and 5 mM *N*-AcHis (30:5) over the time period of approximately 4 hours at pH 4 and 25 °C. The peaks associated with reactants and products are indicated, and the y-axis has been scaled to the highest peak. The x-axis is measured in ppm.

In the top left spectrum of Figure 3.2, two singlets can be seen at approximately 8.65 ppm and 7.3 ppm – these are characteristic of unreacted *N*-AcHis. In the right upper hand spectrum of Figure 3.2, the singlet at approximately 2.02 ppm indicates the acetyl group of *N*-AcHis. The platinum signal has been excluded from the spectrum due to the fact that platinum is in such high concentration that the peak does not change significantly. After only 40 minutes of reaction time at a pH of 4, we see that product peaks have started to evolve. All three of the indicated product signals – at roughly 8.65 ppm, 7.3 ppm, and 1.97 ppm – are indicative of the product, which in this case we believe to be a mono-product coordinated through a Pt-N bond. The rate constant for this reaction was calculated using DYNAFIT and was determined to be $7.2 \pm 0.7 \times 10^{-3}$ M^{-1} s^{-1} [11].

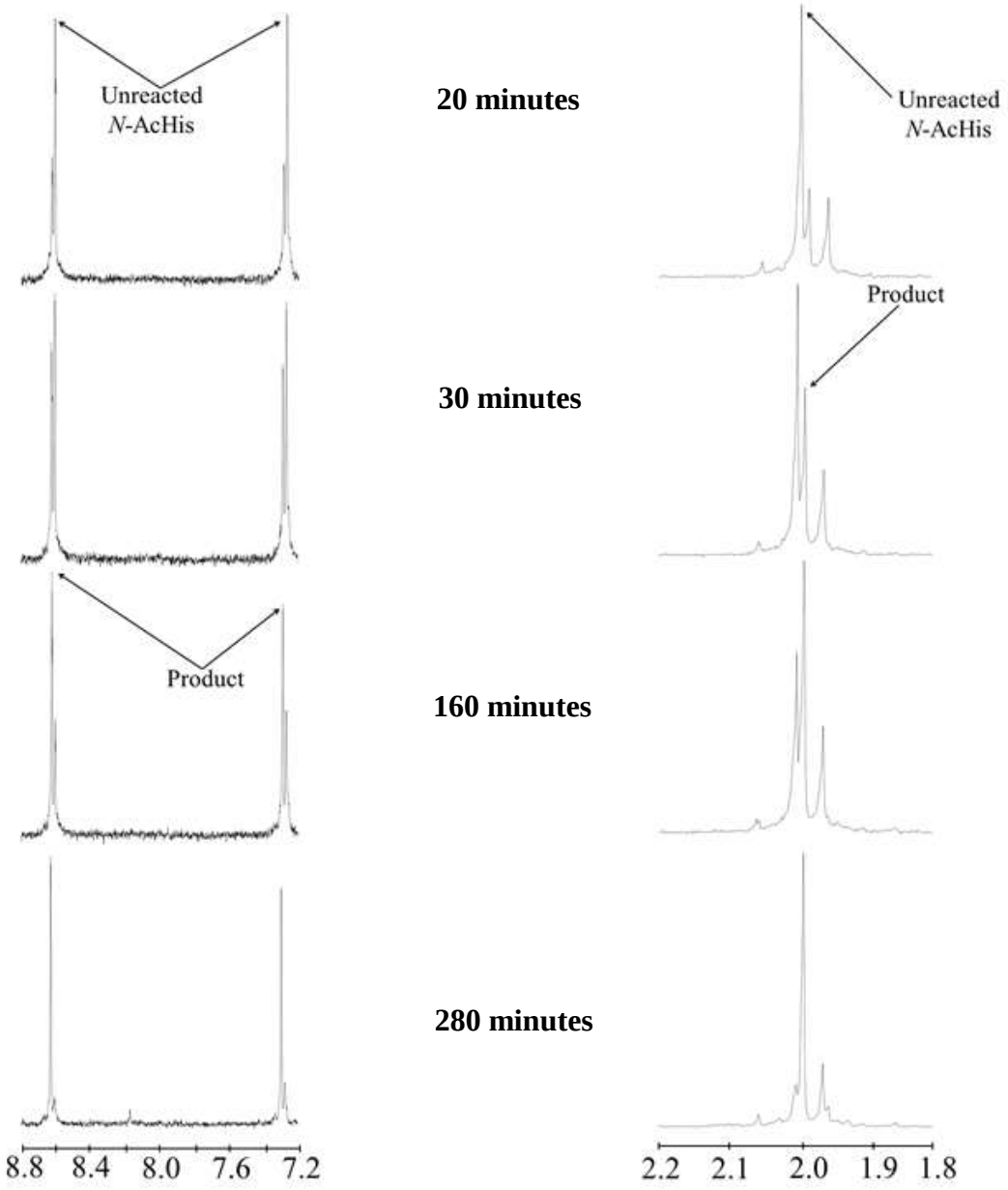

Figure 3.3. The downfield (left) and upfield (right) partial ^{1}H NMR spectra of the reaction of 30 mM Pt(Me_4en)(NO_3)$_2$ and 5 mM *N*-AcHis (30:5) over the time period of approximately 4 hours at pH 4 and 25 °C. The peaks associated with reactants and products are indicated, and the y-axis has been scaled to the highest peak. The x-axis is measured in ppm.

The singlet signals in the top left spectrum of Figure 3.3, seen at approximately 8.65 ppm and 7.3 ppm, are characteristic of unreacted *N*-AcHis. And in the upper right spectrum of Figure 3.3, the signal at approximately 2.02 ppm is associated with the acetyl group of *N*-AcHis. The platinum signal has not been shown in the partial spectrum due to the fact that platinum is in such high concentration that the peak does not change significantly throughout the reaction. After 40 minutes of reaction time, at only a pH of 4, product peaks have started to evolve. All three of the indicated product peaks shown in Figure 3.3 – found at 8.65 ppm, 7.3 ppm, and 2.0 ppm – are associated with the mono-product which we believe to be a mono-product coordinated through the Pt-N bond. The rate constant for this reaction was calculated using DYNAFIT and was determined to be $8.5 \pm 0.6 \times 10^{-3}$ M^{-1} s^{-1} [11].

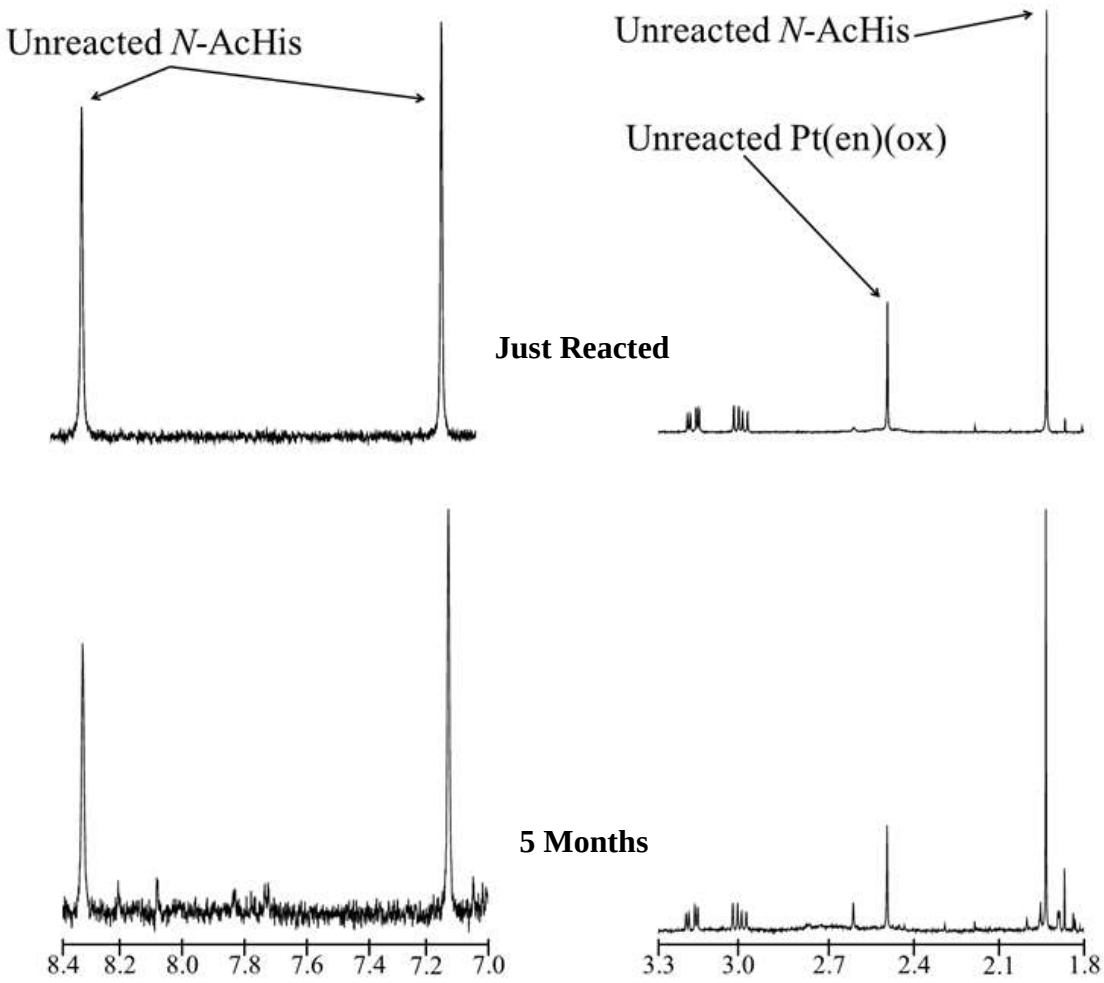

Figure 3.4. The downfield (left) and upfield (right) partial ^{1}H NMR spectra of the reaction of 5 mM Pt(en)(ox) and 5 mM *N*-AcHis (1:1) over the time period of approximately 5 months at pH 7 and approximately 18 °C (room temperature). The peaks associated with reactants are indicated, and the y-axis has been scaled to the highest peak. The x-axis is measured in ppm.

The prominent signals at approximately 8.2 ppm, 7.4 pppm, and 1.95 ppm indicate the presence of unreacted *N*-AcHis, while the signal at approximately 2.5 ppm is characteristic of our platinum compound – Pt(en)(ox). After 5 months of reaction time, no significant reaction was observed. The same reaction sample was checked again via ^{1}H NMR after 14 months of reaction time, only to find very minimal reaction.

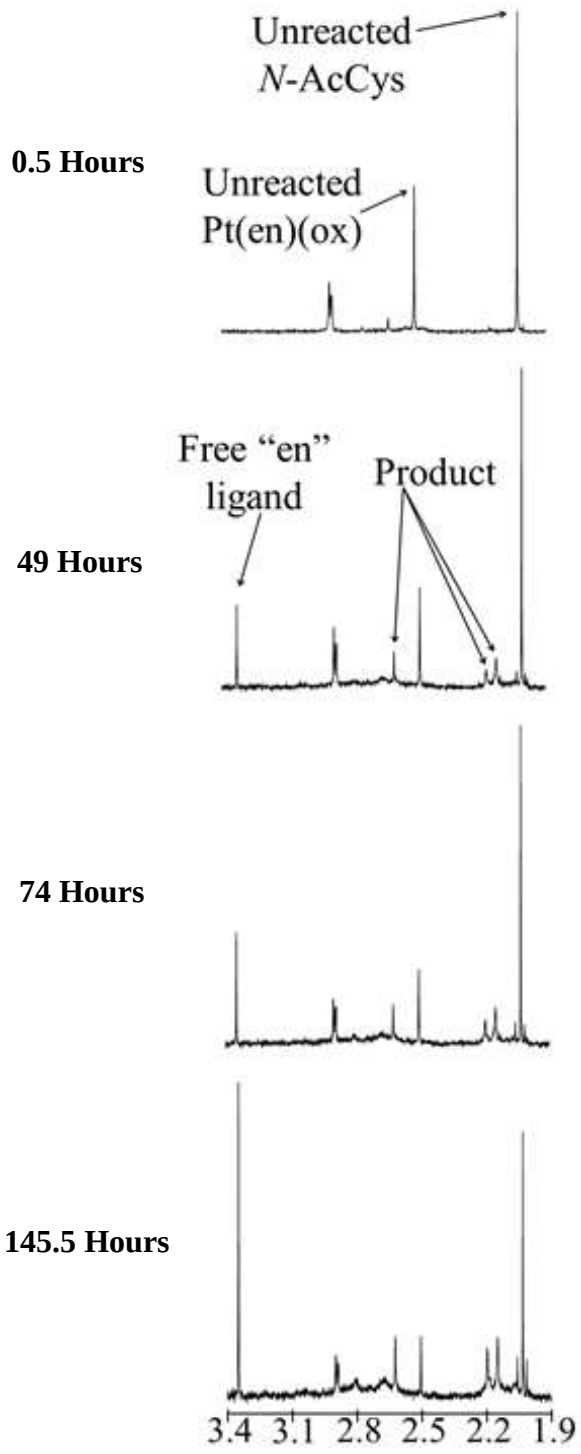

Figure 3.5. Partial ^{1}H NMR spectra of the reaction of 5 mM Pt(en)(ox) and 5 mM *N*-AcCys over the time period of 6 days at pH 7 and approximately 18 °C (room temperature). The peaks associated with reactants, products, and free ligand are indicated, and the y-axis has been scaled to the highest peak. The x-axis is measured in ppm.

The prominent signal at approximately 1.95 ppm is characteristic of *N*-AcCys, and the singlet at roughly 2.5 ppm is associated with our platinum compound – Pt(en)(ox). After 49 hours of reaction time we begin to see product and free en ligand. The singlet peak at roughly 3.35 ppm indicates our free en ligand, and there are three prominent product peaks labeled in Figure 3.5. The singlet peak at approximately 2.65 ppm and the doublet at roughly 2.2 ppm more than likely indicate a bis-chelate product, with two chelated cysteines to one platinum center coordinate through Pt-S and Pt-N bonds. The rate constant for this reaction was estimated using the integration function of the JEOL Delta program and DYNAFIT and was determined to be approximately 2×10^{-4} M^{-1} s^{-1}.

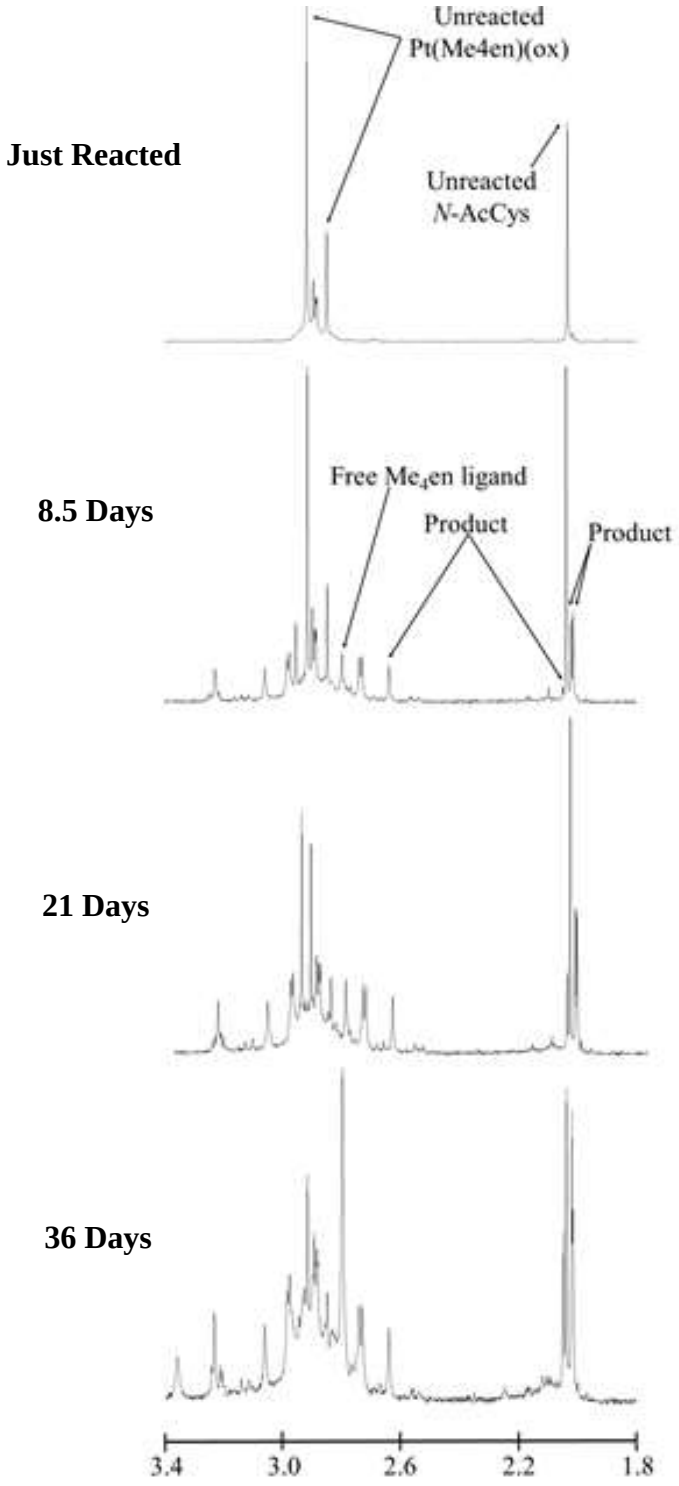

Figure 3.6. Partial ^{1}H NMR spectra of the reaction of 5 mM Pt(en)(ox) and 5 mM *N*-AcCys over the time period of 36 days at pH 7 and approximately 18 °C (room temperature). The peaks associated with reactants, products, and free ligand are indicated, and the y-axis has been scaled to the highest peak. The x-axis is measured in ppm.

The signal at roughly 2.0 ppm is characteristic of *N*-AcCys, while the two prominent singlet peaks indicated in the topmost spectrum of Figure 3.6, located at approximately 3.0 ppm and 2.8 ppm, are indicative of Pt(Me_4en)(ox). After 8.5 days of reaction time we start to see some product formation and free Me_4en ligand. The signal at roughly 2.85 ppm, in conjunction with a singlet noted at approximately 3.6 ppm which is not shown, we known that there is free Me_4en ligand in solution [12]. The doublet shown at approximately 2.0 ppm and the singlet at roughly 2.05 ppm indicate a bis-chelated product of 2 cysteines to one platinum center, coordinate through Pt-S and Pt-N bonds. The rate constant for this reaction was estimated using the integration function of the JEOL Delta program and DYNAFIT and was determined to be approximately 6.5×10^{-5} M^{-1} s^{-1}.

CHAPTER 4

DISCUSSION

We have found that $Pt(en)(NO_3)_2$ in its reaction with *N*-AcMet predominately forms a $[Pt(en)(N\text{-AcMet-S,N})]^+$ chelate. In previous research, it has been shown that this reaction can produce three possible products: $[Pt(en)(N\text{-AcMet-S,N})]^-$, $[Pt(en)(N\text{-AcMet-O,S})]^+$, and/or $[Pt(en)(N\text{-AcMet-S})_2]$ [12]. The first product is likely the more thermodynamically favored in the reaction of 1:1 molar ratio $Pt(en)(NO_3)_2$ and *N*-AcMet, which can be found in **Figure 3.1**, due to the 1:1 ratio. The bis-product in this case is not favorable in a 1:1 reaction, but when there is an excess of *N*-AcMet in 2:1 or greater [12]. The formation of our chelated product is evidenced by the formation of the doublet at approximately 2.3 ppm indicating the hydrogens of the en ligand, and the singlet at 2.45 from the acetyl hydrogens. There may also be evidence of a 1:1 *N*-AcMet:Pt mono-product, but due to the chelate effect and thermodynamic favorability, the chelated product results from this. We believe that the first step in the reaction mechanism is the formation of the $[Pt(en)(N\text{-AcMet-S})(H_2O)]$ product, which is the slowest reaction step; the mono-chelated product, $[Pt(en)(N\text{-AcMet-S,N})]^-$, is then quickly formed. Thus, the reaction rate for this chelation reaction is actually determined by the first step, the formation of the mono-product, and was determined to be $3.8 \pm 0.7\ M^{-1}\ s^{-1}$ [11]. In addition it should be noted that upon bulk addition to the carrier ligand (from en to

Me_4en), the reaction rate was significantly retarded [11]. The ratio of k_{en}/k_{Me4en} was found to be 16, indicating that the reaction rate was slowed by a factor of 16 as sufficient bulk was added to the platinum compound [11].

In the reaction of *N*-AcHis with $Pt(en)(NO_3)_2$ it was found that the dominant product of the reaction was a 1:1 *N*-AcHis:Pt mono-product coordinated through a Pt-N bond. This was still the observed product even when the platinum was in extreme excess in the 30:5 Pt:*N*-AcHis molar ratio observed in **Figure 3.2**. We believe that one reason for the observed sluggishness of the reaction is due to the fact that displacement of the NO_3 ligand by a N is less favorable than the displacement by a S, and thus slower. In addition, the formation of the mono-product and lack of chelated product may be due to the large planar ring of *N*-AcHis, making chelation difficult. This mono-product is evidenced predominately through the production of three product peaks – at roughly 8.65 ppm, 7.3 ppm, and 1.97 ppm – as can be seen in **Figure 3.2**. The singlet at 1.97 ppm is indicative of the acetyl hydrogen of *N*-AcHis, and the other two indicated product singlets represent the imidazole hydrogens. The slight chemical shift between the unreacted *N*-AcHis singlets and the two product singlets at roughly 8.65 ppm and 7.3 ppm is characteristic of a product coordinated through the imidazole nitrogen. In order to verify this we increased the sample from its pH of 4, to 5, 6, and finally 7 in order to determine whether it was coordinated through the imidazole nitrogen. Due to the lack of peak shift as the pH changed, we know that the Pt center is coordinated through the imidazole nitrogen in this product. In addition, a rate constant for the reaction was calculated using DYNAFIT and was found to be $7.2 \pm 0.7 \times 10^{-3}$ M^{-1} s^{-1} [11].

Following this, we developed another platinum drug derivative with a bulkier carrier ligand than the previous experiment, Me_4en, in order to determine how the reaction rate changed. From this reaction of $Pt(Me_4en)(NO_3)_2$ and *N*-AcHis, we can see that the preferred product is again a 1:1 *N*-AcHis:Pt mono-product coordinated through the imidazole nitrogen. As indicated in **Figure 3.3,** we can see that again there are three prevalent product peaks formed at 8.65 ppm, 7.3 ppm, and 2.0 ppm which indicate the previously described product. In this case, since we increased the bulk of the carrier ligand by adding four methyl groups, we hypothesized that the reaction rate would be retarded due to the increased steric hindrance. Surprisingly, we found that there was negligible difference between the rate of the previous reaction, $7.2 \pm 0.7 \times 10^{-3}\ M^{-1}\ s^{-1}$, and this rate of reaction, which was found to be $8.5 \pm 0.6 \times 10^{-3}\ M^{-1}\ s^{-1}$ [11]. While these rates may appear different, the ratio of k_{en}/k_{Me4en} in this case is 1, thus revealing that there is negligible difference between the rates of the two reactions and that bulk addition has no effect with *N*-AcHis [11].

Following this, we wished to investigate the change in the rate of reaction as we increased the bulk of the platinum compound leaving ligand from nitrate to oxalate. In this case we first wanted to observe the 1:1 reaction of *N*-AcHis and Pt(en)(ox) at pH7 and room temperature (18 °C). After roughly 2 weeks of reaction time, there was still no product formation, so we opted to just let the reaction run, checking it periodically for reaction. Finally after about 5 months, a miniscule amount of product was observed, and even after 14 months of reaction there was only a small amount of product formation. The partial ^1H NMR spectra from this reaction can be seen in **Figure 3.4** and indicate this lack of product formation. Originally, we also desired to observe the 1:1 reaction of *N*-

AcHis and Pt(Me_4en)(ox), but once we realized how slow the previous reaction had proceeded, we knew that it would be an incredibly time-consuming process to try to observe this reaction as well. In addition, we deemed these reactions too slow to have any biological relevance due to the likelihood that the platinum drug will have reacted with something else well before this reaction would take place.

Upon observing the reaction of *N*-AcCys and Pt(en)(ox), which we knew would be much faster than that of the *N*-AcHis reaction, the dominant product was found to be a 2:1 *N*-AcCys:Pt bis-chelate of [Pt(*N*-AcCys-S,$N)_2$] even when the original reaction mixture was 1:1. This is further supported by the findings that selenomethionine (SeMet), a nonstandard amino acid, was found to form a bis-chelated product [Pt(SeMet-Se,$N)_2$] [13]. Thus it seems logical to follow that both *N*-AcMet and *N*-AcCys are able to form a bis-chelated product, and thus [Pt(*N*-AcCys-S,$N)_2$] is a likely product of the reaction of *N*-AcCys and Pt(en)(ox). As seen in **Figure 3.5**, the singlet at roughly 2.65 ppm and the doublet at 2.2 ppm indicate the formation of this product. The singlet is associated with the *N*-AcCys acetyl group and the doublet corresponds to the other protons of the *N*-AcCys portion of the product. This bis-chelate product is further confirmed by the presence of free en ligand in solution, which indicates that the carrier ligand has been knocked off of the platinum and has been replaced. The removal of the chelated oxalate carrier ligand and the following formation of the bis-chelate product is thermodynamically favorable and thus is very probable product; this phenomenon can be explained by examining the proposed reaction mechanism. The reaction of the first cysteine is very slow, but upon reaction with cysteine a S-Pt bond is formed and the chelation of the oxalate is broken, leaving a mono-dentate oxygen behind. This allows

for the reaction of the second cysteine to take place quickly, forming another Pt-S bond, because the mono-dentate oxygen is not as stable as the chelated oxalate and thus is easily replaced. It should be noted that we believe the reaction of a second cysteine occurs more quickly than the S,N-chlelation seen in previous reactions due to the preference of S over N by Pt. Once two cysteines are coordinated to the platinum center, the chelated en ligand is replaced with two chelated cysteines; this is favorable because one chelate is being replaced by two chelates. In addition, we found that this 1:1 reaction of Pt(en)(ox) and *N*-AcCys takes approximately 6 days to reach completion and the estimated rate of reaction is roughly 2×10^{-4} M^{-1} s^{-1}.

In order to understand how this reaction rate is affected by bulk addition to the carrier ligand, the 1:1 reaction of *N*-AcCys and Pt(Me_4en)(ox) at pH 7 and 18 °C was observed. Upon product formation, we see a doublet at approximately 2.0 ppm and singlets at roughly 2.65 ppm and 2.05 ppm, which are again indicative of our bis-chelate product [Pt(*N*-AcCys-S,N)$_2$]. In this case, the reaction took approximately 36 days to reach completion and the rate was found to be 6.5×10^{-5} M^{-1} s^{-1}. From the ratio of k_{en}/k_{Me4en}, found to be approximately 3, we see that the reaction of the Me_4en compound is roughly 3-fold slower with *N*-AcHis than is the en compound.

It is interesting that in the case of *N*-AcHis, the addition of substantial bulk to the carrier ligand of the platinum compound does not affect the rate of reaction, but in the cases of both *N*-AcMet and *N*-AcCys the reaction is significantly affected by bulk addition. This is an extremely substantial finding because it suggests that by adding sufficient bulk to the platinum compound the preferred protein target could potentially be changed from methionine or cysteine, both sulfur-containing targets, to histidine, a non-

sulfur-containing target, or possibly another biomolecule. These results could have major implications in reducing toxic side effects for the patient as well as increasing anticancer effectiveness.

REFERENCES

[1] American Cancer Society. Cancer Facts & Figures 2014. Atlanta: American Cancer Society; 2014.

[2] O'Dwyer, P. J.;Stevenson, J. P.; Johnson, S. W. Clinical Status of Cisplatin, Carboplatin, and Other Platinum-Based Antitumor Drugs. In Cisplatin – Chemistry and Biochemistry of a Leading Anticancer Drug; Lippert, B., Ed.; Verlag Helvetica Chimica Acta, WILEY-VCH: Zürich, 1999; 31-69.

[3] Rosenberg, B. Platinum Complexes for the Treatment of Cancer: Why the Search Goes On. In Cisplatin – Chemistry and Biochemistry of a Leading Anticancer Drug; Lippert, B., Ed.; Verlag Helvetica Chimica Acta, WILEY-VCH: Zürich, 1999; 3-27.

[4] Wang, D; Lippard, S. J. *Nature Reviews* **2005**, *4*, 307-320.

[5] Wheate, N. J.; Walker, S.; Craig, G. E.; Oun, R. *Dalton Transactions* **2010**, *39*, 8113-8127.

[6] Carboplatin. American Cancer Society. [Online]. Available: http://www.cancer.org/treatment/treatmentsandsideeffects/guidetocancerdrugs/carboplatin. Accessed: 10/17/2014.

[7] Alderman, R. A.; Hall, M. D.; Hambley, T. W. *Journal of Chemical Education* **2006**, *83*, 728-734.

[8] Howell, S. B.; Safaei, R.; Larson, C.; Sailor, M. J. *Molecular Pharmacology* **2010**, *77*, 887-894.

[9] Zamble, D. B.; Lippard, S. J. The Response of Cellular Proteins to Cisplatin-Damaged DNA. In Cisplatin – Chemistry and Biochemistry of a Leading Anticancer Drug; Lippert, B., Ed.; Verlag Helvetica Chimica Acta, WILEY-VCH: Zürich, 1999; 73-110.

[10] Esteban-Fernández, D.; Moreno-Gordaliza, E.; Cañas, B.; Palacios, M. A.; Gómez-Gómez, M. M. *Metallomics* **2010**, *2*, 19-38.

[11] R. S. Sandlin; C. J. Whelan; M. S. Bradley; K. M. Williams. *Inorganica Chimica Acta* **2012**, *391*, 135-140.

[12] Williams, K. M.; Rowan, C.; Mitchell, J. *Inorganic Chemistry* **2004**, *43*, 1190-1196.

[13] Williams, K. M.; Dudgeon, R. P.; Chmely, S. C.; Robey, S. R. *Inorganica Chimica Acta* **2011**, *368*, 187-193.